

# Influence of the Shear Layer Thickness on the Flow Around Unsteady Airfoils

Alexander Widmann and Cameron Tropea

**Abstract** Experiments with a pitching and plunging unsteady airfoil have been conducted in order to investigate the influence of the separating shear layer properties on the formation and detachment of leading edge vortices (LEVs). The chord length was varied from 90 to 180 mm keeping all non-dimensional parameters constant. It has been shown, that the mechanism of vortex detachment changes with chord length, manifested by a change in flow topology. One mechanism scales with chord length, the other is attributed to viscous effects in the boundary layer. For this mechanism a new scaling of the LEV circulation is introduced.

## 1 Introduction

The timing of the formation and detachment of leading edge vortices (LEV) has according to McCroskey [15] a strong impact on the lift and drag values of an unsteady airfoil. The detachment of LEVs is linked in the literature to an interaction with the trailing edge. In this case the chord length  $c$  is the characteristic quantity for the limitation of the LEV. The most common concept for predicting the LEV circulation is the concept of optimal vortex formation introduced by Gharib et al. [11] and extended to flapping flight by Dabiri [4]. It has been confirmed experimentally by Rival et al. [17] or Baik et al. [2]. For a wide range of applications, a non-dimensional maximum circulation of  $T^* = \frac{\Gamma}{cU} \approx 4$  is predicted, suggesting universal applicability (with  $\Gamma$  as the LEV circulation,  $c$  as the airfoil chord length and  $U$  as the free stream velocity). Authors like Baik et al. [2], Jones and Babinsky [13], Rival et al. [18] or DeVoria and Ringuette [5] find disagreement with their results. Therefore, the present

---

A. Widmann (✉) · C. Tropea  
Institute of Fluid Mechanics and Aerodynamics, Technische Universität Darmstadt,  
Flughafenstr. 19, 64347 Griesheim, Germany  
e-mail: a.widmann@iesy.net

C. Tropea  
e-mail: ctropea@sla.tu-darmstadt.de

study has the goal of examining the mechanisms of LEV formation and detachment in more detail and over a greater range of operation parameters.

Basically two mechanisms are conceivable for LEV detachment, one relying on the chord length and the other one relying on the viscous/inviscid interaction of the vortex and the airfoil. The former is referred to as a bluff body detachment mechanism, the latter as boundary-layer eruption.

The bluff body vortex detachment mechanism depends on the size of the LEV attached to the airfoil, its development is shown Fig. 1.

The LEV is confined by two half saddles, one at the leading edge where the shear layer feeding into the LEV separates, the second is the LEV's reattachment point and moves further downstream as the LEV grows. If this point reaches the trailing edge, it merges with the stagnation point at the rear part of the airfoil and forms a full saddle point  $S$  in the free stream. According to Rival et al. [19] this full saddle enables a flow reversal at the trailing edge: fluid containing counter-clockwise vorticity ( $\omega^+$ ), which is of opposite rotation as the LEV, interacts with the shear layer containing clockwise vorticity ( $\omega^-$ ) and causes the LEV to be 'cut off'. This mechanism is analogous to the vortex detachment mechanisms for bluff bodies explained by Gerrard [10] and agrees with Roshko [20], who identifies the wake width of a bluff body as the characteristic length for vortex shedding.

The eruption driven mechanism is inherent to any vortex/wall configuration and is independent of any geometrical length scale. Doligalski et al. [7] explain this mechanism as the viscous response of a boundary layer to the imposed pressure gradient by a vortex. The LEV induces a velocity relative to the airfoil surface, which is maximal just below its core and decreases towards the stagnation point at the leading edge. Therefore an adverse pressure gradient is imposed on the boundary layer, which separates from the airfoil surface as soon as the pressure gradient and the induced velocity reach a critical value.

The boundary-layer separation leads to the ejection of vorticity carrying fluid out of the boundary layer, which accumulates and forms a secondary vortex. A scheme for this mechanism is given in Fig. 2. At first, Fig. 2a shows an attached vortex prior to the boundary-layer separation. The LEV is given by node  $N_1$  and confined by a streamline passing through the half saddle points  $S'_3$  and  $S'_4$ . The stagnation points on the pressure side and at the trailing edge are given by  $S'_1$  and  $S'_2$ . Figure 2b shows the situation after the LEV has grown, the boundary layer has separated from the surface at the half saddle  $S'_6$  and forms a secondary vortical structure with the node  $N_2$ . According to the

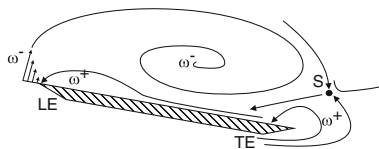


**Fig. 1** LEV detachment from a flat plate corresponding to the bluff body detachment mechanism with a full saddle point and flow reversal at the trailing edge

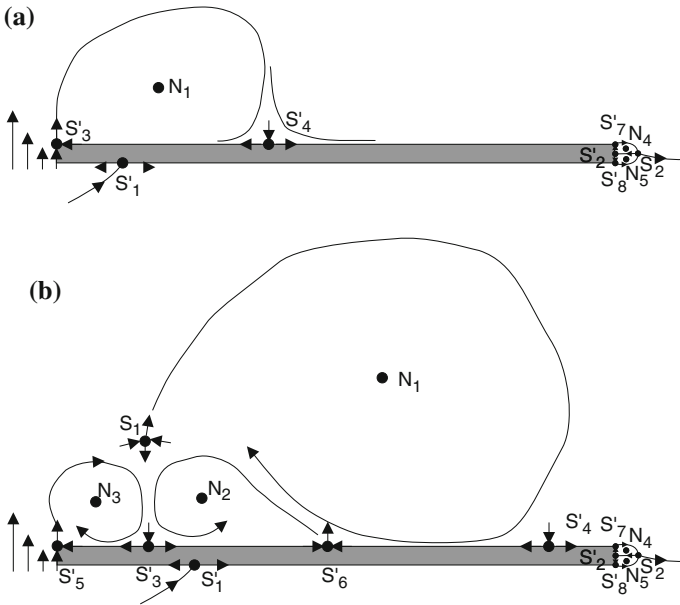


**Fig. 2** Topological representation of the eruption driven vortex detachment mechanism transferred to the case of an unsteady airfoil. **a** Flow topology prior boundary-layer separation, **b** flow topology after boundary-layer separation

topological considerations of Foss [9], the sum of nodes  $N$  and saddles  $S$  in a fixed flow domain kept is constant. The mathematical rule for the topological description of an open ended plane intersecting a solid body (which represents the experimental case) is given by Tobak and Peak [23]:  $(\sum 2N + \sum N') - (\sum 2S + \sum S') = -2$ . Therefore the formation of a secondary vortex with a node requires the formation of subsequent node  $N_3$  and saddle points  $S'_5$  and  $S_1$  to fulfill the topological constraints. A tertiary vortex ( $N_3$ ) with the same rotation direction as the LEV and a full saddle ( $S_1$ ) forms. The full saddle redistributes the vorticity carrying fluid emerging from the shear layer: It is not fed into the primary LEV, but into the tertiary vortex, which in turn starts growing while the primary LEV does not accumulates any more circulation.

Both mechanisms already show the importance of the leading edge shear layer on LEV formation and detachment. On the one hand, an interaction of secondary flow structures with the shear layer causes LEV detachment in both previously explained concepts. A shear layer with higher velocity gradients seems to be more resilient against this interaction, as suggested in Rival et al. [17] or [19]. On the other hand, the growth rate of the LEV in terms of mass and circulation is determined by the shear layer properties, if the ideas of Kaden [14] are considered, who argues that the fluid emerging from the shear layer is directly advected into the LEV. Because the LEV circulation and its distance to the solid wall (given by its diameter) determine the boundary-layer eruption, it is plausible that the shear layer effects the LEV detachment directly. As a first-order approximation Didden [6] and Roshko [20]

express the circulation increase of the LEV  $\dot{\Gamma}$  as the integration of vorticity  $\omega$  over the shear layer thickness  $d_{SL}$ , given by Eq. 1, with  $U(y)$  as the velocity profile over the shear layer. The shear layer vorticity is approximated as  $\omega \approx -\frac{\partial U}{\partial y}$  with  $y$  as the wall normal distance. The approximated mass flux  $\dot{m}$  according to Kaden [14] is given in Eq. 2.

$$\dot{\Gamma} = \int_{y=0}^{d_{SL}} \omega(y)U(y) dy \approx \frac{1}{2}U^2 \quad (1)$$

$$\dot{m} = \rho \int_{y=0}^{d_{SL}} U(y) dy \approx \frac{1}{2}\rho U d_{SL} \quad (2)$$

While the mass flux  $\dot{m}$  into the LEV directly depends on the shear layer thickness  $d_{SL}$ , the circulation increase  $\dot{\Gamma}$  is independent of  $d_{SL}$ . If one assumes that the shear layer emerges from the stagnation point on the pressure side of the airfoil and moves around the leading edge where it finally separates from the surface, its thickness  $d_{SL} = 2.4\sqrt{\frac{\nu}{a}}$  may be approximated by the Falkner-Skan equation taken from Schlichting and Gersten [22], with  $\nu$  is the kinematic viscosity and  $a = \frac{U(x,y)}{x} = -\frac{V(x,y)}{y}$  as a constant describing the local flow field in the vicinity of a stagnation point. The ratio of circulation and contained mass varies for an LEV according to the shear layer properties and the free stream velocity. This concept is in agreement with the considerations of Betz [3], who emphasizes the impact of the shear layer thickness on vortex formation.

Usually, an airfoil in unsteady motion is sufficiently described by the non-dimensional parameters Reynolds number  $Re = \frac{Uc}{\nu}$ , Strouhal number  $St = \frac{2\Delta h}{UT}$  and reduced frequency  $k = \frac{\pi c}{UT}$  for a fixed angle of attack history  $\alpha_{eff}(t/T)$ , with the chord length  $c[m]$ , the free stream velocity  $U[\frac{m}{s}]$ , its plunging height  $\Delta h[m]$ , its motion frequency or motion period  $f = \frac{1}{T}[\frac{1}{s}]$  and the kinematic viscosity  $\nu[\frac{m^2}{s}]$ . This perspective neglects viscous effects such as the boundary layer eruption. For the extreme case of a semi-infinite chord length, the LEV cannot grow infinitely but the bluff body shedding mechanism is also inhibited, because no flow reversal can occur. In such a case the boundary layer eruption leads to LEV detachment. Consequently, a chord length needs to exist, which provokes a transition in the detachment mechanisms. If the dimensional parameters of an unsteady airfoil are varied in a way to keep the non-dimensional parameters constant, the shear layer thickness cannot be kept constant and varies with  $d_{SL} \propto U^{-0.5}$ , while  $c \propto U^{-1}$ . The shear layer thickness breaks the similarity between the experimental cases. This article describes the experimental observation of a pitching and plunging sharp edged flat plate, for which the chord length is increased successively from  $c = 90$  mm to  $c = 180$  mm in order to observe a transition in the LEV detachment mechanism, while the non-dimensional parameters are kept constant. A very low Reynolds number of  $Re = 16875$  has been chosen to highlight viscous effects and a large reduced frequency of  $k = 0.5$  has been chosen to underline unsteady effects. The Strouhal number  $St = 0.25$  was fixed to a value representative for efficient forward flight.

## 2 Experimental Setup

Particle image velocimetry (PIV) was used to investigate the flow field created by pitching and plunging flat plates in the Eiffel-type wind-tunnel of Technische Universität Darmstadt. The airfoil motion was selected in such a way that for different chord lengths  $c = [90; 120; 150; 180]$  mm the non-dimensional parameters  $Re$ ,  $k$ ,  $St$  and  $\alpha_{eff}(t/T)$  remain constant for the different test cases  $A$ ,  $B$ ,  $C$  and  $D$ . Five independent runs were executed per test case. Therefore the free stream velocity  $U$ , the plunging height  $\Delta h$ , the motion period  $T$  and the pitch angle have been adjusted accordingly. An overview over the dimensional parameters of the four test cases  $A$ ,  $B$ ,  $C$  and  $D$  is given in the Table 1 below. A schematic description of the airfoil kinematic motion is given in Fig. 3. A combined pitching and plunging motion leads to the separation of the boundary layer at the leading edge and subsequent roll-up of the shear layer into a distinct vortex. Linear actuators with a spacing of  $s = 80$  mm create the plunging motion. In the two diagrams of this figure the airfoil is depicted right at the beginning of the stroke at  $t_1$  (top) and later in the stroke cycle at  $t_2$  (bottom). The camera’s field of view  $FOV$  is given by the dashed rectangle. The airfoils spanned from wall to wall, creating nominally two-dimensional conditions. While their chord lengths varied from case to case, their thickness and leading edge shape remained constant. Figure 4 schematically shows the flat plate profiles used in the study. The leading and trailing edge were sharp with an angle of  $\Theta = 30^\circ$ , ensuring a well defined separation location. The plate thickness was  $d = 6$  mm. The pivot point of the pitch movement was placed at the leading edge to prevent the effective angle of attack to be influenced by the pitch rate of the profile.

### 2.1 Data Processing

The vorticity in the flow field cannot be exclusively attributed to a single flow structure, therefore a vortex identification scheme introduced by Graftieaux et al. [12] was applied to allocate circulation to the occurring vortical flow structures. The scalar fields  $\Gamma_1$  and  $\Gamma_2$  are derived from the velocity data and used to asses whether a part of the field is part of a vortical structure. IAs (interrogation areas), in which these scalars exceed their threshold values of  $|\Gamma_1| = 0.9$  and  $|\Gamma_2| = 0.6$ , are identified as part of

**Table 1** Dimensional experimental parameters of the four test cases

Test case	$c$ [mm]	$U_\infty$ [ $\frac{m}{s}$ ]	$T$ [ms]	$\Delta h$ [mm]
A	90	3.0	95	71
B	120	2.25	167	94
C	150	1.8	262	118
D	180	1.5	377	141

**Fig. 3** Schematic representation of the combined pitching and plunging motion

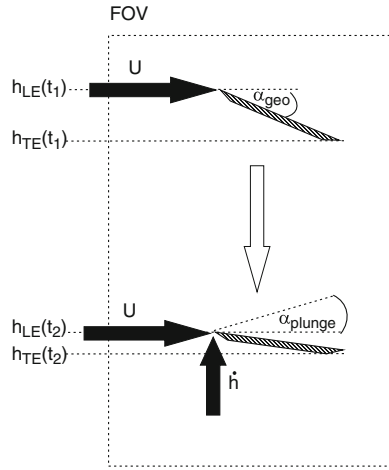
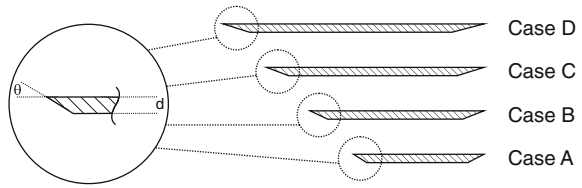
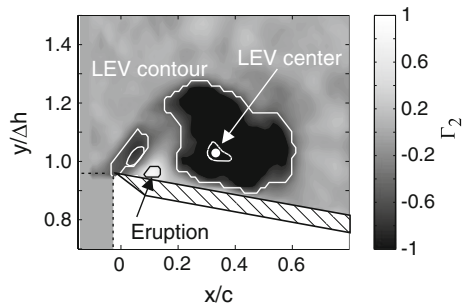


**Fig. 4** Geometry of the flat plates in the four experimental cases



a vortical structure. Figure 5 gives an example of the identified vortical structures near the airfoil leading edge. The scalar  $\Gamma_2$  is color coded, the contours of the vortex core and center are marked. The area covered by the LEV and its center are marked, additionally the secondary vortex caused by the boundary layer eruption is identified and the rolling up tertiary vortex directly at the leading edge. According to Fage and Johansen [8] the LEV detachment is defined as the instant, when a self-contained vortical structure is no longer fed any more circulation through the shear layer and therefore reaches a peak value. The rear reattachment point *XRP* of the vortex is estimated by tracking the rear most saddle point in the flow field.

**Fig. 5** Example of the identified vortical structures in the flow field above the airfoil



### 3 Results

The results of the PIV measurements are shown in Fig. 6 for independent time resolved experimental runs. The instantaneous streamlines and the color coded normalized vorticity  $\omega^* = \frac{\omega c}{U}$  is given for non-dimensional time steps in the plunging motion  $t/T = [0.18; 0.22; 0.26; 0.30]$ . Negative vorticity appears blue, positive vorticity red. The regions below and upstream of the airfoil were masked out due to shadowed regions. As the motion phase  $t/T$  increases, a layer of positive vorticity forms below the LEV on the suction side of the airfoil due to the no-slip condition.

Subsequently secondary structures emerge from this layer leading to LEV detachment and a full saddle in the free stream above the leading edge can be found. This full saddle initiates the LEV detachment by a redistribution of fluid emerging from the shear layer into the tertiary structure. While a secondary structure at the leading edge of the airfoil for case *A* appears only after the LEV rear attachment point has moved beyond the trailing edge, in the cases *B*, *C* and *D* the evolution of such a structure is already present before the LEV rear attachment point has reached the trailing edge. For the time step  $t/T = 0.26$  in case *A* the reversed flow from the trailing edge below the LEV containing positive vorticity is clearly visible, prior to that no secondary structures appear in the flow field. In contrast, this flow reversal does not occur in the cases *B*, *C* and *D* until the LEV has detached from the airfoil. This indicates that the boundary has separated independently of any length scales related to the airfoil chord. The temporal evolution of the non-dimensional LEV circulation  $\frac{\Gamma^{LEV}}{cU}$ , the circulation of the secondary structure  $\frac{\Gamma^{Eruption}}{cU}$  and the position of the rear reattachment point  $\frac{X_{RPP}}{c}$  were calculated from the experimental data. Figure 7 shows the normalized LEV circulation for a motion period of  $t/T = 0.1 - 0.5$ . The instants in time for which the rear LEV reattachment point reaches the trailing edge  $\frac{X_{RPP}}{c} = 1$  is marked by a vertical dashed line, its standard deviation is 5 % of the chord length at most. The standard deviation is shown in form of error bars. The non-dimensional times when  $X_{RPP} = c$  are different throughout all experimental cases and shifted towards earlier times for shorter chord lengths, indicating smaller LEV

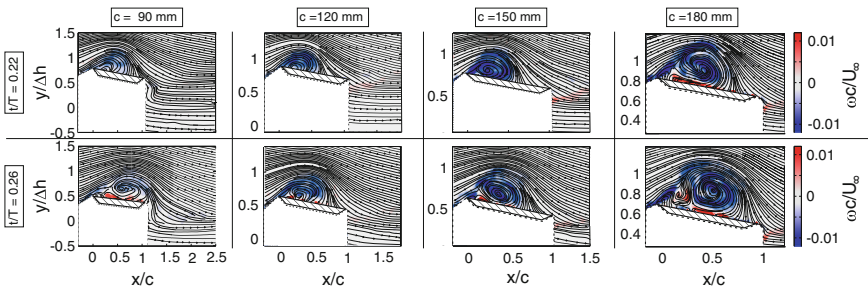


**Fig. 6** Flow field development in terms of normalized vorticity and streamlines for each experimental case at  $t/T = [0.22; 0.26]$

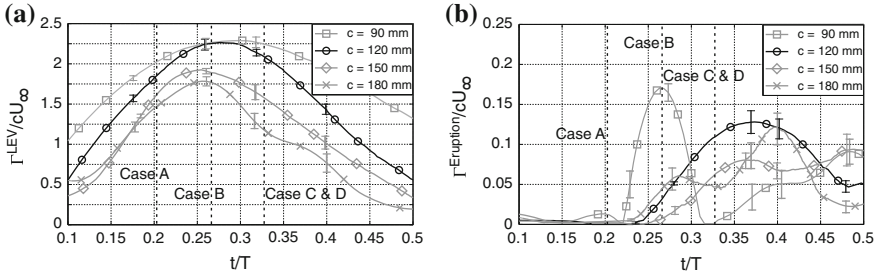


**Fig. 7** Chord based normalized circulation development of the LEV and the boundary layer eruption zone. **a** LEV circulation, **b** eruption circulation

sizes with respect to the chord length with increasing free stream velocities, due to thinner shear layers, which agrees with the theoretical considerations in Sect. 1.

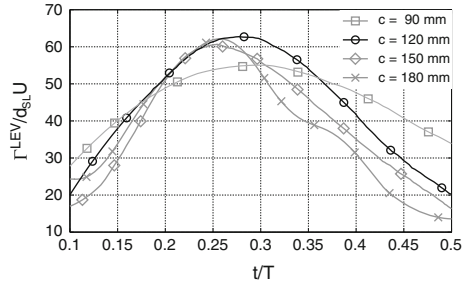
All LEV circulation curves in Fig. 7a exhibit the same trend with a circulation increase from the start of the motion ( $t/T = 0$ ) to approximately the middle of the stroke ( $t/T \approx 0.25$ ), where a peak value is reached and a subsequent drop can be observed. The peak values of the normalized LEV circulation decrease with increasing chord length. Although the non-dimensional parameters of all experimental cases are kept constant, the circulation curves do not collapse. A completely different behavior is observed for the circulation development of the secondary vortical structures in Fig. 7b. For case A the secondary vortical structure exhibits a peak early in the stroke cycle, which immediately follows the flow reversal at the trailing edge. In contrast, for all other cases the formation of the secondary structures coincides with (case B) or even precedes (cases C and D) the excess of the rear reattachment point beyond the trailing edge, indicating that the formation of the secondary vortical structure is independent of the chord length. These observations suggest that different mechanisms lead to the LEV detachment in case A and cases C and D. Since both events roughly coincide in case B, the detachment may be a mixture of both mechanisms.

### 3.1 Shear Layer Based Normalization

For the eruption driven LEV detachment mechanism cases (C and D, perhaps B),  $d_{SL}$  is suspected to determine the LEV size. An alternative normalization method  $\frac{\Gamma^{LEV}}{d_{SL}U}$  based on the shear layer properties is tested.  $a_0$  was calculated using potential flow theory. The flow field around the airfoil in unsteady motion is expressed by potential flow theory. The velocity data in the vicinity of the stagnation point at the highest angle of attack obtained with this method is used to determine  $a$  after the definition given by Schlichting [22]  $a = \frac{U}{x} = \frac{-V}{y}$ . Subsequently,  $a$  was divided by the free



**Fig. 8** Normalized LEV circulation based on the shear layer properties:  $\frac{\Gamma^{LEV}}{d_{SL}U}$



stream velocity to obtain  $a_0 = \frac{a}{U}$ . Values of  $a_0 = [2.77; 2.78; 2.75; 2.76]$  1/m with a respective standard deviation of  $\sigma(a_0) = [6.40; 6.48; 5.82; 5.76]$  % are found for all four cases. In all cases  $a_0$  was uniform in the region around the stagnation point implying the correctness of the assumptions. The alternative normalization of the LEV circulation curves using the shear layer thickness is shown in Fig. 8. It can be seen, that the circulation curves coincide for the cases B, C and D which can be attributed to the boundary-layer eruption, but fails for case A where the LEV detaches due to the bluff body mechanisms. With decreasing vorticity in the shear layer ( $\propto d_{SL}^{-1}$ ) the LEV has to accumulate more mass to achieve the same circulation. If a Reynolds number based on the LEV circulation  $Re_{LEV} = \frac{\Gamma^{LEV}}{\nu}$  is defined, it decreases (and therefore promotes viscous effects like the boundary layer eruption) with decreasing free stream velocity  $U$ , as can be seen in Fig. 7a.

### 4 Conclusion

It was shown, that a transition in the LEV detachment mechanisms could be facilitated by a change in the chord length. The influence of the chord length on the formation and detachment of LEVs has been investigated, while keeping all non-dimensional parameters constant. Two different LEV detachment mechanisms were observed for the four experimental cases: For one mechanism the chord length was the characteristic geometrical length scale limiting LEV growth, for the other mechanism no geometrical length scale was found to be associated with LEV detachment, which is in accordance with Sattari et al. [21], Afanasyev [1], or Pedrizzetti [16]. This viscous inviscid wall-vortex interaction is inherent to all vortex-airfoil configurations. The shear layer properties determining the circulation/mass ratio in an LEV was found to be characteristic for the maximal LEV circulation.

## References

1. Afanasyev, Y.D.: Formation of vortex dipoles. *Phys. Fluids* **18**, 037103 (2006)
2. Baik, Y.S., Bernal, L.P., Granlund, K., Ol, M.V.: Unsteady force generation and vortex dynamics of pitching and plunging aerofoils. *J. Fluid Mech.* **709**, 1–32 (2012)
3. Betz, A.: Wie entsteht ein Wirbel in einer wenig zhen Flüssigkeit? *Die Naturwissenschaften* **37**, 193–196 (1950)
4. Dabiri, J.O.: Optimal vortex formation as a unifying principle in biological propulsion. *Annu. Rev. Fluid Mech.* **41**, 17–33 (2009)
5. DeVoria, A.C., Ringuette, M.J.: Vortex formation and saturation for low-aspect-ratio rotating flat-plate fins. *Exp. Fluids* **52**, 441–462 (2012)
6. Didden, N.: On the formation of vortex rings: rolling-up and production of circulation. *J. Appl. Math. Phys.* **30**, 101–115 (1979)
7. Doligalski, T.L., Smith, C.R., Walker, J.D.: Vortex interactions with walls. *Annu. Rev. Fluid Mech.* **26**, 573–616 (1994)
8. Fage, A., Johansen, F.C.: XLII. The structure of vortex sheets. *Lond. Edinb. Dublin Philos. Mag. J. Sci.* **5**, 417–441 (1928)
9. Foss, J.F.: Surface selections and topological constraint evaluations for flow field analyses. *Exp. Fluids* **37**, 883–898 (2004)
10. Gerrard, J.H.: The mechanics of the formation region of vortices behind bluff bodies. *J. Fluid Mech.* **25**, 401–413 (1966)
11. Gharib, M., Rambod, E., Shariff, K.: A universal time scale for vortex ring formation. *J. Fluid Mech.* **360**, 121–140 (1998)
12. Graftieaux, L., Michard, M., Grosjean, N.: Combining PIV, POD and vortex identification algorithms for the study of unsteady turbulent swirling flows. *Meas. Sci. Technol.* **12**, 1422–1429 (2001)
13. Jones, A.R., Babinsky, H.: Unsteady lift generation on rotating wings at low Reynolds numbers. *J. Aircr.* **47**, 1013–1021 (2010)
14. Kaden, H.: Aufwicklung einer unstablen Unstetigkeitsfläche. *Ing. Arch.* **2**, 140–168 (1931)
15. McCroskey, W.J.: Unsteady airfoils. *Annu. Rev. Fluid Mech.* **14**, 285–311 (1982)
16. Pedrizzetti, G.: Vortex formation out of two-dimensional orifices. *J. Fluid Mech.* **655**, 198–216 (2010)
17. Rival, D.E., Prangemeier, T., Tropea, C.: The influence of airfoil kinematics on the formation of leading-edge vortices in bio-inspired flight. *Exp. Fluids* **46**, 823–833 (2008)
18. Rival, D.E., Manejev, R., Tropea, C.: Measurement of parallel blade-vortex interaction at low Reynolds numbers. *Exp. Fluids* **49**, 89–99 (2010)
19. Rival, D.E., Kriegseis, J., Schaub, P., Widmann, A., Tropea, C.: Characteristic length scales for vortex detachment on plunging profiles with varying leading-edge geometry. *Exp. Fluids* **55**, 1–8 (2014)
20. Roshko, A.: On the Drag and Shedding Frequency of Two-Dimensional Bluff Bodies—Technical Note 3169. National Advisory Committee for Aeronautics (1954)
21. Sattari, P., Rival, D.E., Martinuzzi, R.J., Tropea, C.: Growth and separation of a start-up vortex from a two-dimensional shear layer. *Phys. Fluids* **24**, 1–14 (2012)
22. Schlichting, H., Gersten, K.: *Boundary Layer Theory*. Springer, Berlin (2001)
23. Tobak, M., Peak, D.J.: Topology of three-dimensional separated flows. *Annu. Rev. Fluid Mech.* **14**, 61 (1982)